Journal of Inclusion Phenomena and Molecular Recognition in Chemistry **31:** 243–264, 1998.

SL_2 Type Phase Solubility Diagrams, Complex Formation and Chemical Speciation of Soluble Species

MOHAMMAD B. ZUGHUL
Department of Chemistry, University of Jordan, Amman, Jordan.

ADNAN A. BADWAN
The Jordanian Pharmaceutical Manufacturing Company, P.O. Box 94, 11710 Naor, Jordan

(Received: 23 July 1997; in final form: 1 October 1997)

Abstract. A method is presented for the analysis of SL_2-type phase solubility diagrams. The method allows the determination of individual complex formation and solubility product constants through rigorous fitting of all segments of the diagram: the rising portion, the plateau and the descending portion. Rigorous analysis of the descending portion offers the means of discerning the type of complex precipitate (SL or SL_2).

The method has been tested by computer simulation of experimental data for both SL and SL_2 complex precipitates. The limits of precision of experimental data required to obtain reasonable estimates of equilibrium constants have been explored through superimposition of statistical random noise. The method has also been successfully applied to the analysis of some experimentally measured phase solubility diagrams that have been reported in the literature. These include the measured solubilities of 1,3-dimethylbenzoylurea (DMBU) against catechol concentration in carbon tetrachloride, tolbutamide (Tolb) against aqueous β-cyclodextrin concentration, spironolactone (SP) against aqueous γ-cyclodextrin concentration, in addition to methylparaben, ethylparaben and propylparaben against aqueous α-cyclodextrin concentration at 25 °C.

Key words: SL_2 type phase solubility diagrams, complex formation, chemical speciation, cyclodextrin.

1. Introduction

Since Higuchi and Connors published their classical, exemplary review on phase solubility techniques [1], including details on the types and shapes of phase solubility diagrams, a wealth of experimental information has been released on the extent of solubility enhancement, of essentially water-insoluble compounds, by aqueous solutions of various solubilizers.

One major class of these diagrams belongs to solute (S) – solubilizer (L) systems forming SL_2-type complexes. A significant number of these systems demonstrate a rising portion, a plateau and a descending portion in their phase solubility diagrams [1–8]. Analysis of these diagrams to obtain the partial formation constants K_{11} and K_{12} of soluble complexes SL and SL_2, respectively, has largely been developed for the rising portion of the phase diagrams [9–13]. They ranged from rigorous explicit

simple expressions that can be applied to reasonably precise experimental data in the rising portion [9–11], to more involved models applying some approximations regarding the relative magnitude of partial formation constants K_{11} and K_{12} [14, 15]. No rigorous analysis of the descending portion of SL_2-type phase diagrams has been published, aside from an approximate application of one single data point to obtain a rough estimate of K_{12} [1, 2, 6]. A recently published article [16] dealt with a rigorous analysis of S_2L-type phase diagrams. Since the descending portion of the diagram offers more information on the type of complex precipitate (SL or SL_2) than can be provided by the rising portion, which only involves soluble complexes, an attempt was made in this work to develop a complete rigorous method for analysis of all segments of SL_2-type phase diagrams. Further, testing of this method to simulated and experimental data is reported.

2. Theoretical Treatment

Referring to Figure 1, which depicts a typical phase solubility diagram for an SL_2-type complex, the *solubility* of the solute S_{eq} is plotted against the *initial stoichiometric concentration of the solubilizer* L_t to produce the curve S_0–a–b–c. For the purpose of establishing rigorous modeling of the various equilibria involved in soluble complex formation, complex saturation and precipitation, the diagram refers to measurements of S_{eq} following the addition of equal amounts of the solute S_t to a series of aqueous solutions of the solubilizer differing in L_t. S_t must be in excess of the *optimum saturation solubility* S_m. Following equilibrium, S_{eq} is measured while the corresponding *equilibrium concentration of the solubilizer* L_{eq} is either measured or estimated for each solution. This is met by having $S_t > S_m$ and $L_t > L_m$ for solute – solubilizer systems yielding a solid complex precipitate beyond saturation; L_m being the equilibrium solubilizer concentration corresponding to S_m. For systems having only soluble complexes over the entire range of measurements, the phase diagram will only show the rising portion of the diagram, and the analysis corresponding to that portion will also be valid. In what follows is a breakdown of the procedure followed by analysis of each region of the phase diagram which leads to the evaluation of formation and solubility product constants from linear and nonlinear fitting of experimental data.

The complex equilibria involved over the entire range of the phase solubility diagram covering regions I, II and III of Figure 1 are:

$$S_{(eq)} + L_{(aq)} \rightleftharpoons SL_{(eq)}, \quad K_{11} = [SL]/[S][L] \tag{1}$$

$$L_{(eq)} + SL_{(aq)} \rightleftharpoons SL_{2(eq)}, \quad K_{12} = [SL]_2/[L][SL] \tag{2}$$

where K_{11} and K_{12} define the equilibrium partial formation constants of SL and SL_2 complexes, respectively. The overall formation constant of the SL_2 complex is of course given by $\beta_{12} = K_{11}.K_{12} = [SL_2]/[S][L]^2$.

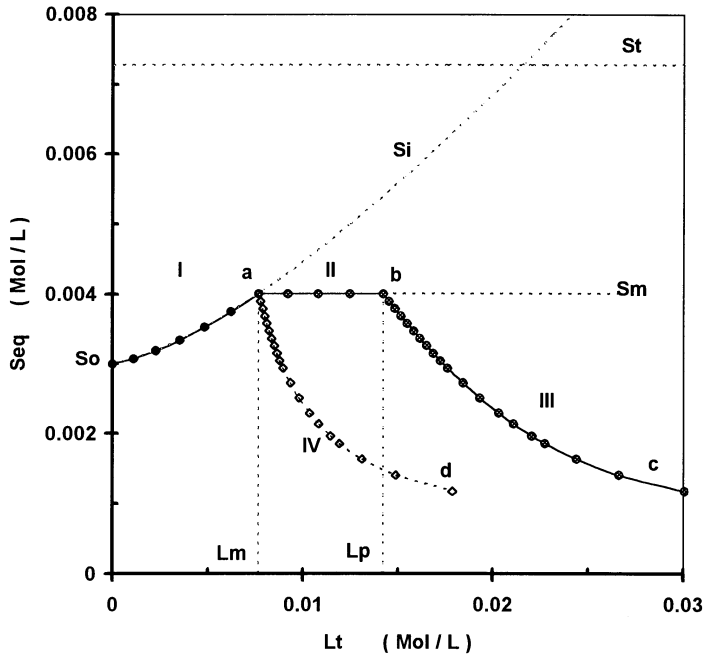

Figure 1. A typical SL_2-type phase solubility diagram obtained for an SL_2-complex precipitate having S_o = 3 × 10^{-3} M, S_m = 4.008 × 10^{-3} M, L_m = 7.656 × 10^{-3} M, K_{11} = 20 M^{-1}, K_{12} = 300 M^{-1}, K_{S12} = 1.088 × 10^{-7} M^3, S_t = 7.28 × 10^{-3} M and L_p = 0.0142. The phase diagram resulting from a plot of S_{eq} against L_t is denoted by the three regions I, II and III. That resulting from a plot of S_{eq} against L_{eq} is denoted by regions I and IV. S_t depicts the solubility expected from the rising portion (region I) in the absence of complex precipitation (i.e., supersaturation).

2.1. REGION I

Only soluble complexes (SL and SL_2) are formed in this region, and since the solid solute is present in excess at equilibrium with free solute species, it follows that [S] = S_o and

$$S_{eq} - S_o = [SL] + [SL_2] = K_{11}S_o[L](1 + K_{12}[L]) \tag{3}$$

$$L_{eq} = [L] + [SL] + 2[SL_2] = [L]\{1 + K_{11}S_o(1 + K_{12}[L])\} = L_t, \tag{4}$$

Subtraction of twice Equation (3) from Equation (4), followed by rearrangement yields the following expression for the free solubilizer concentration [9, 13]

$$[L] = Q/(1 - K_{11}S_o \tag{5}$$

where

$$Q = L_t - 2(S_{eq} - S_o). \tag{6}$$

Substitution for [L] from Equation (5) into Equation (3) yields:

$$S_{\text{eq}} - S_{\text{o}} = QK_{11}S_{\text{o}}\{1 + K_{12}Q/(1 - K_{11}S_{\text{o}})\}/(1 - K_{11}S_{\text{o}}). \tag{7}$$

This, when divided by Q, leads to the linear relation:

$$y = a + b.Q \tag{8}$$

where $y = (S_{\text{eq}} - S_{\text{o}})/Q$, $a = K_{11}S_{\text{o}}/(1 - K_{11}S_{\text{o}})$ and $b = aK_{12}/(1 - K_{11}S_{\text{o}})$. Thus plotting y against Q yields a straight line with intercept a and slope b, from which rough estimates of the complex formation constants are obtained according to:

$$K_{11} = a/\{S_{\text{o}}(1 + a)\} \tag{9}$$

$$K_{12} = b(1 - K_{11}S_{\text{o}})/a. \tag{10}$$

These rough estimates may be used as first guesses in the subsequent analysis of the descending portion of the phase diagram.

2.2. REGION II

This region occurs following saturation of the solution with both the solid solute and the complex whose solid precipitate remains at equilibrium with the liquid phase. The system is characterized by having three components ((C = 3) and three phases (liquid solution + solid solute + solid complex, all at equilibrium and thus $p = 3$), so the number of degrees of freedom $f = C - p + 2 = 2$, which are temperature and pressure. Since both T and P are fixed, the system is invariant and thus the concentrations of all soluble species remain fixed each at [S] = S_{o}, [L] = [L_{m}], [SL] = $[\text{SL}]_{\text{m}} = K_{11}S_{\text{o}}[\text{L}_{\text{m}}]$, $[\text{SL}_2] = [\text{SL}_2]_{\text{m}} = K_{11}K_{12}S_{\text{o}}[\text{L}_{\text{m}}]^2$ and hence

$$\begin{aligned} S_{\text{eq}} &= S_{\text{o}} + [\text{SL}]_{\text{m}} + [\text{SL}_2]_{\text{m}} = S_{\text{o}} + K_{11}S_{\text{o}}[\text{L}_{\text{m}}] + K_{11}K_{12}S_{\text{o}}[\text{L}_{\text{m}}]^2 \\ &= S_{\text{m}} \end{aligned} \tag{11}$$

$$\begin{aligned} L_{\text{eq}} &= [\text{L}_{\text{m}}] + [\text{SL}]_{\text{m}} + 2[\text{SL}_2]_{\text{m}} = [\text{L}] + K_{11}S_{\text{o}}[\text{L}_{\text{m}}] + 2K_{11}K_{12}S_{\text{o}}[\text{L}_{\text{m}}]^2 \\ &= L_{\text{m}}. \end{aligned} \tag{12}$$

The subscript m denotes species in the plateau region, where S_{m} and L_{m} are obtained from the intersection of the rising portion (region I) with the plateau (region II) shown in Figure 1, while [L_{m}] is the corresponding concentration of free solubilizer species. Region II appears as a horizontal plateau so long as S_{t} remains in excess of the maximum solubility S_{m} subject to either of the two following constraints:

Case (a): For an SL_2-complex precipitate: $S_t \geq S_m + 0.5(L_t - L_m)$; $L_t > L_m$
Case (b): For an SL-complex precipitate: $S_t \geq S_m + (L_t - L_m)$; $L_t > L_m$.

In either case, the concentration of free solubilizer species [L_m] is obtained from Equation (12) according to:

$$[L_m] = [-K_{11}S_o + \{(K_{11}S_o)^2 + 4K_{11}K_{12}S_o(S_m - S_o)\}^{1/2}]/2K_{11}K_{12}S_o. \tag{13}$$

2.3. REGION III

The descending portion of the phase solubility diagram is obtained when the solute is initially added in excess of S_m, but not in sufficient excess to leave any trace of solid solute in equilibrium with the liquid phase. This implies that either complex, SL or SL_2, will precipitate at the expense of free solute species in solution. This requires the concentration of the free solute species [S] to decrease while that of the free solubilizer species [L] to increase subject to either of the two following constraints:

Case (a). The solution is saturated with SL_2-type complex and is at equilibrium with its solid precipitate subject to the constraint: $S_m \leq S_t < S_m + 0.5(L_t - L_m)$; $L_t > L_m$.

The concentration of its soluble form is held constant throughout region III at its same concentration of region II, i.e., $[SL_2] = [SL_2]_m = K_{11}K_{12}[S][L]^2 = K_{11}K_{12}S_o[L_m]^2$ and hence the concentration of free solute [S] and free solubilizer [L] both vary subject to the constraint

$$[S] = S_o[L_m]^2/[L]^2. \tag{14}$$

The stoichiometric concentration of solubilizer is given by

$$L_{eq} = [L] + [SL] + 2[SL_2]_m = [L] + K_{11}[S][L] + 2K_{11}K_{12}S_o[L_m]^2. \tag{15}$$

Now, substituting for [S] from Equation (14) into (15) and solving for [L] yields

$$[L] = 0.5\{a_1 + (a_1^2 - 4b_1)^{1/2}\} \tag{16}$$

where $a_1 = L_{eq} - 2K_{12}b_1$ and $b_1 = K_{11}S_o[L_m]^2$.

Substituting for [L] from Equation (16) into Equation (14) yields [S], both of which are used to compute the predicted equilibrium solute concentrations

$$S_{eq}^P = [S]\{1 + K_{11}[L](1 + K_{12}[L])\} \tag{17}$$

which are then used in nonlinear least squares fitting to obtain the minimum of sum of squares of differences SSQ given by:

$$\text{SSQ} = \sum (S_{\text{eq}} - S_{\text{eq}}^{P})^2. \tag{18}$$

In this fitting procedure, initial estimates (guesses) may normally be obtained from analysis of region I according to Equation (8) if the number and precision of experimental data in that region is sufficient to allow reasonable estimates. This is most often not the case especially when the rising portion data appear rather scattered and almost linear and thus allows only an estimate of the so called *apparent formation constant* K given by

$$K = T/\{S_{\text{o}}(1 - T)\} \tag{19}$$

where T is the slope of the rising portion assumed to be linear. In this case it was found practical to plug in the initial guesses $K_{11} \approx K$ and $K_{12} = 0$ subject to the constraints: $K_{11} \geq 0$ and $K_{12} \geq 0$.

A typical nonlinear least squares fitting algorithm available in most PC statistical packages apply the Marquardt–Levenberg finite difference routine for minimizing SSQ (SPSSIPC^{+}, Version 5.0, SPSS, Inc., 444 N. Michigan Avenue, Chicago, Illinois 60611). This routine proved efficient in converging to a unique minimum yielding reproducible estimates of the formation constants.

In those cases where L_{eq} is not measured but only L_{t} is known, L_{eq} is estimated for data fitting according to

$$L_{\text{eq}} = L_{\text{t}} - (L_{\text{p}} - L_{\text{m}}) - 2(S_{\text{m}} - S_{\text{eq}}); \quad L_{\text{t}} > L_{\text{m}} \tag{20}$$

where L_{p} is obtained from the intersection of regions II and III.

Case (b). The solution is saturated with SL-type complex and is at equilibrium with its solid precipitate subject to the constraint: $S_{\text{m}} < S_{\text{t}} < S_{\text{m}} + (L_{\text{t}} - L_{\text{m}})$; $L_{\text{t}} > L_{\text{m}}$.

The concentration of SL thus remains constant at its same value of region II, i.e., $[\text{SL}] = [\text{SL}]_{\text{m}} = K_{11}[\text{S}][\text{L}] = K_{11}S_{\text{o}}[\text{L}_{\text{m}}]$ and hence the concentrations of free solute [S] and free solubilizer [L] both vary subject to the condition

$$[\text{S}] = S_{\text{o}}[\text{L}_{\text{m}}]/[\text{L}] \tag{21}$$

while the concentration of soluble SL_2-type complex varies according to $[\text{SL}_2] = K_{11}K_{12}[\text{S}][\text{L}]^2 = K_{11}K_{12}S_{\text{o}}[\text{L}_{\text{m}}][\text{L}]$. Substituting for [S] from Equation (21), the stoichiometric concentration of solubilizer in this region (III) is given by

$$L_{\text{eq}} = [\text{L}] + [\text{SL}]_{\text{m}} + 2[\text{SL}_2] = [\text{L}] + K_{11}S_{\text{o}}[\text{L}_{\text{m}}] + 2K_{11}K_{12}S_{\text{o}}[\text{L}_{\text{m}}][\text{L}]. \tag{22}$$

Which upon rearrangement and solving for [L] yields

$$[\mathrm{L}] = (L_{\mathrm{eq}} - K_{11}S_{\mathrm{o}}[\mathrm{L_m}])/(1 + 2K_{11}K_{12}S_{\mathrm{o}}[\mathrm{L_m}]). \tag{23}$$

Substituting for [L] from Equation (23) and for [S] from Equation (21), $S^{\mathrm{P}}_{\mathrm{eq}}$ is readily calculated for each solution according to

$$S^{\mathrm{P}}_{\mathrm{eq}} = [\mathrm{S}] + [\mathrm{SL}]_{\mathrm{m}} + [\mathrm{SL_2}] = [\mathrm{S}] + K_{11}S_{\mathrm{o}}[\mathrm{L_m}] + K_{11}K_{12}S_{\mathrm{o}}[\mathrm{L_m}][\mathrm{L}] \tag{24}$$

and SSQ is minimized according to Equation (18) to obtain estimates of K_{11} and K_{12} from the best data fit as shown earlier.

If the equilibrium concentration of solubilizer (L_{eq}) was not measured but only L_{t} is known, then the following relation

$$L_{\mathrm{eq}} = L_{\mathrm{t}} - (L_{\mathrm{p}} - L_{\mathrm{m}}) - (S_{\mathrm{m}} - S_{\mathrm{eq}}) \tag{25}$$

holds and may be used to fit the experimental data for an SL-type complex precipitate. To ascertain whether an SL-complex reaches saturation first, instead of an SL_2-complex, a plot of ($S_{\mathrm{eq}}L_{\mathrm{eq}}$) against ($S_{\mathrm{eq}} + L_{\mathrm{eq}}$) for data of region III will appear quite linear for an SL-complex precipitate. However, the same plot will be nonlinear with a pronounced positive curvature for an SL_2-complex precipitate. To illustrate this point, substitution for S_{eq} and L_{eq} from Equations (24) and (22), respectively, and ignoring a combination of positive and negative higher order terms in $[\mathrm{L}]^2$ and $[\mathrm{L}][\mathrm{L}_m]$ (which almost cancel each other for various K_{11}/K_{12} ratios) yields the approximately linear relation: $S_{\mathrm{eq}}L_{\mathrm{eq}} \approx a_2 + b_2(S_{\mathrm{eq}} + L_{\mathrm{eq}})$ where $a_2 \approx K_{\mathrm{S11}} - b_2^2$ and $b_2 \approx K_{11}K_{\mathrm{S11}}$.

For a solute-solubilizer system forming an SL-complex only with no higher order complexes, substitution of $K_{12} = [\mathrm{SL_2}] = 0$ into Equations (24) and (22) for data of region III leads to the exact relation:

$$S_{\mathrm{eq}}L_{\mathrm{eq}} = a_2 + b_2(S_{\mathrm{eq}} + L_{\mathrm{eq}}) \tag{26}$$

where $a_2 = K_{\mathrm{S11}} - b_2^2$ and $b_2 = K_{11}K_{\mathrm{S11}}$. Thus a plot of ($S_{\mathrm{eq}}L_{\mathrm{eq}}$) against ($S_{\mathrm{eq}} + L_{\mathrm{eq}}$) for data of region III will be exactly linear with an intercept a_2 and slope b_2 from which K_{11} and K_{S11} are obtained according to:

$$K_{\mathrm{S11}} = a_2 + b_2^2 \tag{27}$$

$$K_{11} = b_2/K_{\mathrm{S11}}. \tag{28}$$

The value of K_{11} thus obtained should (within reasonable bounds of experimental error) be equal to the apparent formation constant K, obtained from analysis of region I according to Equation (19), while $[\mathrm{L_m}]$ and L_{eq} are given by:

$$[L_{\mathrm{m}}] = L_{\mathrm{m}}/(1 + K_{11}S_{\mathrm{o}}) \tag{29}$$

$$L_{\text{eq}} = L_{\text{t}} - (L_{\text{p}} - L_{\text{m}}). \tag{30}$$

Use of these latter relations will also be demonstrated in the analysis of simulation as well as experimental data to differentiate between systems forming only SL-complexes, from those forming SL_2-complexes with either an SL-complex precipitate, or an SL_2-complex precipitate.

3. Results and Discussion

3.1. Simulation results

Figure 1 shows a typical phase solubility diagram for a solute–solubilizer system forming an SL_2-type complex which reaches saturation first. The diagram corresponds to a system with the following properties: S_{o} = 3 × 10^{-3} M, K_{11} = 20 M^{-1}, K_{12} = 300 M^{-1}, S_m = 4.008 × 10^{-3} M, L_{m} = 7.656 × 10^{-3} M, L_{P} = 0.0142 M, S_{t} = 7.28 × 10^{-3} M and K_{S12} = 1.088 × 10^{-7} M^3. Aqueous solutions of the solubilizer used were within the range $0 \leq L_{\text{t}} \leq 3 \times 10^{-2}$ M with an equal amount of excess solid solute S_{t} = 9.5 × 10^{-2} M added to each.

Usually, the rising portion of the phase diagram is not linear [1], but has a positive curvature (or negative curvature in some systems) which may be suspected of being linear in experiments having relatively large errors, and thus lead to an erroneous estimation of formation constants. If the system forms an SL_2-type complex, then both SL and SL_2 complexes formed are soluble in this region (region I; $S_{\text{o}} - a$), where excess solid solute is at equilibrium with the solution and thus [S] = S_{o}. Rough estimates of the formation constants K_{11} and K_{12} may sometimes be obtained from the linear plot of Equation (8). However, these estimates are usually poor; they most often yield overestimates of K_{11} and negative values of K_{12} due to imprecise data and erroneous determination of S_{o} which is usually obtained through simple linear regression of region I.

Region II (a–b of Figure 1) representing the plateau occurs following saturation of the solution with SL_2 complex, which begins to precipitate thus fixing the concentrations of all soluble species. This is so since the solution is simultaneously at equilibrium with both excess solute and complex SL_2, and thus the solute solubility is fixed at S_{m}, while the corresponding stoichiometric equilibrium concentration of solubilizer is also fixed at L_{m}. The concentration of free solute is S_{o}, and that of free solubilizer species [L_{m}] is obtained from Equation (13), and hence $[\text{SL}]_{\text{m}}$ and $[\text{SL}_2]_{\text{m}}$ are fixed.

In region III (b–c of Figure 1), depicting the descending portion of the phase diagram, it appears when S_{t} is less than that required to maintain excess solid solute in equilibrium with solution. The solid complex SL_2 keeps precipitating at the expense of free solute and thus remains at equilibrium with the solution. This means that both [S] and [L] vary subject to the interrelationship stated by the identity (14) and thus [SL] varies, but $[\text{SL}_2]$ remains equal to $[\text{SL}_2]_{\text{m}}$.

The curve depicted as region IV (a–d in Figure 1) represents a plot of S_{eq} against L_{eq} instead of L_t for data of both regions II and III. The displacement ($L_t - L_{eq}$) is simply equal to twice the effective concentration of the SL_2 complex precipitating from solution for each data point along regions II and III. The dashed curve labeled S_i extending from region I depicts the solubility for a supersaturated solution.

Dependent on the relative magnitudes of formation constants K_{11} and K_{12}, and also on the value of S_o, the rising portion of the phase diagram may appear with a positive curvature ($K_{12} \gg K_{11}$), with a negative curvature ($K_{12} \ll K_{11}$) or almost linear when K_{12} is significantly small. For a limited solubility and/or a limited number of data points, region I may appear practically linear, and hence the system may be suspected of forming either SL or S_2L-type complexes instead of SL_2. To explore these factors and the limits of precision required to allow reasonable estimates of formation and solubility product constants, over the entire range of the phase diagram, the following simulation studies were performed.

Figure 2a depicts the phase diagram for an SL_2-system precipitating SL_2-complex with the following parameters: S_o = 0.003 M, K_{11} = 100 M^{-1}, K_{12} = 70 M^{-1}, $S_m = 5.556 \times 10^{-3}$ M, $S_t = 9.5 \times 10^{-3}$ M, $L_m = 9.312 \times 10^{-3}$ M, L_p = 0.0172 M, and $K_{S12} = 1.08 \times 10^{-7}$ M^3. Note how the rising portion appears almost linear, the slope of which, T = 0.275 with a correlation coefficient r = 0.9993, yields an apparent formation constant K = 128.5 M^{-1} and S_o = 0.00295 M. If region I is analyzed according to Equation (8), it will yield values for K_{11} = 103.37 M^{-1} and K_{12} = 68.77 M^{-1} using the extrapolated value of S_o = 0.00295 M. This indicates that knowledge of the true solubility at zero solubilizer concentration is important in arriving at good estimates of formation constants. When the true value S_o was used, the corresponding true values of formation constants were actually obtained, yet this was the situation for precise input data.

In order to examine the effect of experimental data precision on estimates of K_{11}, K_{12} and S_o, phase diagrams were constructed to which statistical random noise was superimposed. The random noise (RN) was varied from 0 to 5% of the maximum solubility S_m in 1% units. Region I of each diagram was analyzed according to Equation (8) to obtain estimates of K_{11} and K_{12}. Moreover, regions II and III were fitted according to Equations (13), (16) and (18) to obtain the corresponding best estimates. The results for fitting of region III are listed in Table I for each phase diagram. Estimates of S_o, T and K that are listed in the table are those obtained from linear fitting of region I, S_m from region II, whereas K_{11} and K_{12} are those from nonlinear fitting of region III using the corresponding values of S_o listed. The percentage error in estimates of S_o, S_m, K_{11} and K_{12} are also provided for a 95% confidence level. Note, for example, how the slope of the rising portion T varies as % RN varies from 0 to 5%. Though the correlation coefficient only varies slightly from 0.9993 down to 0.9898 on going from 0 to 5% RN, T varies from 0.275 down to 0.251 with a corresponding variation in S_o from 0.00295 up to 0.003072. This results in the estimates of K to vary from 128.5 down to 109.2 M^{-1}. When this value of K was used as an initial guess for K_{11}

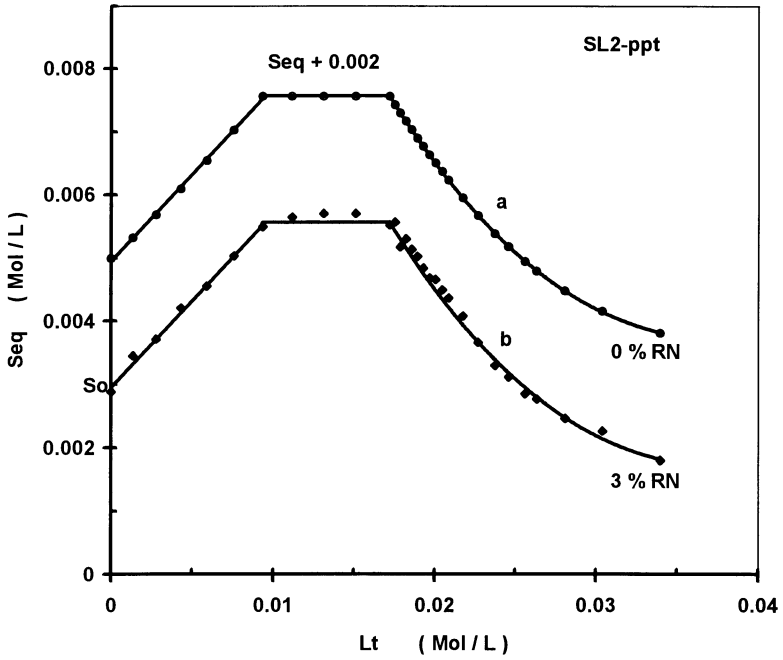

Figure 2. Phase solubility diagram for an SL_2 system precipitating an SL_2-complex having $S_o = 3 \times 10^{-3}$ M, $K_{11} = 100$ M^{-1}, $K_{12} = 70$ M^{-1}, $S_m = 5.556 \times 10^{-3}$ M, $S_t = 9.5 \times 10^{-3}$ M, $L_m = 9.312 \times 10^{-3}$ M, $L_p = 0.0172$ M, $K_{S11} = 1.8 \times 10^{-7}$ M^3. (a) No random noise superimposed; (b) 3% random noise superimposed. In each case, the solid line through the data points represents the best fit from linear and nonlinear regression (Equations 8, 13, 16–18).

while K_{12} was guessed equal to zero in the nonlinear least squares fitting of region III, the corresponding estimates of K_{11} and K_{12} listed in the last two rows were obtained. Note how estimates of K_{11} consistently decrease as % RN increases from 0 to 5%, whereas the percentage error changes from 1.89% through a lower value of 0.812% and up to 5.71%. The variation in K_{12} estimates show the same trend except for a relatively higher percentage error ranging from 0.80% at 0% RN up to 7.32% at 5% RN. This indicates that errors (scatter) in experimental data exceeding 3% of the optimal solubility S_m would yield percentage errors in estimates of K_{12} exceeding 5% when the number of the data points is 20.

Figure 2b shows the same diagram depicted in Figure 2a except for a 3% RN superimposed but displaced by 0.002 M concentration units for comparison. In either case, the solid line indicates the best possible fit obtained.

The same procedure was also followed for analysis of SL_2-type phase diagrams for which an SL-complex precipitates instead of SL_2. Figure 3 shows the corresponding phase diagram obtained with the same parameters of S_o, K_{11}, K_{12}, S_m S_t, L_m and L_p used for Figure 2, except for having an SL-complex precipitate with a solubility product $K_{S11} = 1.8 \times 10^{-5}$ M^2. This was intended in order to examine the effect of the type of complex precipitate on the general shape of region

Table I. The results of parameter estimates obtained from nonlinear least squares fitting of data for an SL_2-type phase solubility diagram (with an SL-complex precipitate) to which 0%, 1%, 2%, 3%, 4% and 5% random noise (RN) was superimposed.

		Retrieved parameter estimates following nonlinear least squares fitting % Random noise (RN) superimposed					
Parameter	Input data	0%	1%	2%	3%	4%	5%
S_o (M)	0.003	−0.00295	0.002975	0.0029990	0.003023	0.003048	0.003072
(% error)		(1.67)	(0.83)	(0.03)	(0.77)	(1.60)	(2.40)
S_m (M)	0.005556	0.005556	0.005566	0.005577	0.005587	0.005598	0.005608
(% error)		(0.00)	(0.11)	(0.38)	(0.56)	(0.75)	(0.94)
T		0.274979	0.270238	0.265498	0.260757	0.256017	0.251276
(r)		(0.9993)	(0.9988)	(0.9976)	(0.9958)	(0.9932)	(0.9898)
K (M^{-1})		128.5	124.5	120.5	116.7	112.9	109.2
K_{11} (M^{-1})	100	101.8918	101.7545	99.18776	97.69273	96.73834	94.29023
(% error)		(1.89)	(1.75)	(0.812)	(2.31)	(3.26)	(5.71)
K_{12} (M^{-1})	70	70.56242	66.90343	66.20806	65.81732	65.55394	64.87284
(% error)		(0.80)	(4.42)	(5.42)	(5.98)	(6.35)	(7.32)

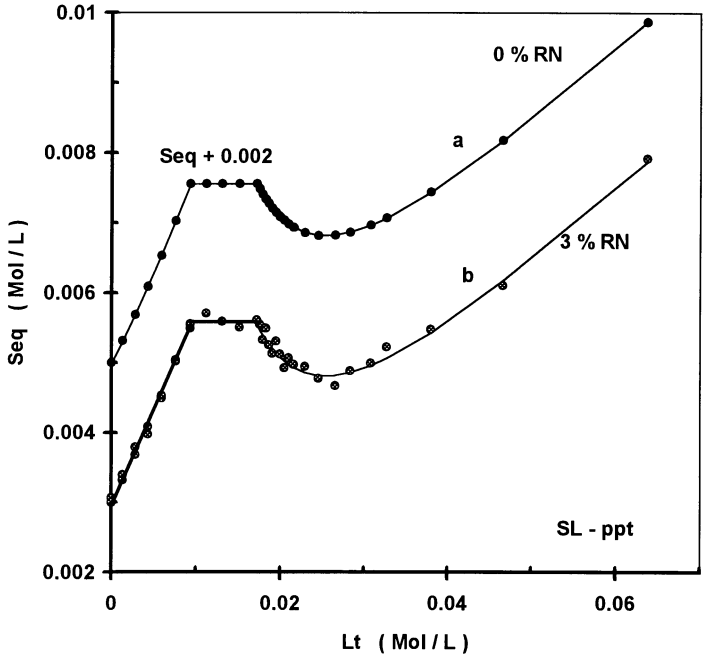

Figure 3. Phase solubility diagram of an SL_2-system precipitating an SL-complex. The same parameters of Figure 2 were retained except for $K_{S11} = \times\ 10^{-5}$ M^2 to replace K_{S12}. (a) No random noise was superimposed; (b) 3% random noise was superimposed. In each case, the solid line represents the best data fit obtained through Equations (8), (13), (18), (23) and (24).

III, and on the precision with which K_{11} and K_{12} are estimated, other conditions being equal. Note how the descending portion begins to rise at sufficiently high L_t concentrations for an SL-complex precipitate but continues to go steadily down for an SL_2-complex precipitate system. This is one characteristic feature which has unnecessarily been ascribed earlier to possible formation of higher order complexes [1]. Random noise was also superimposed ranging from 0 to 5% of S_m and the results of parameter estimates obtained are listed in Table II.

Since regions I and II are identical for Figures 2 and 3, Table II reproduces the same parameter estimates for S_o, T, K and S_m listed in Table I. On the other hand, estimates of K_{11} and K_{12} obtained from analysis of region III show different trends in their percentage errors as a function of % RN superimposed. For example, though estimates of K_{11} consistently decrease as before, the error decreases from 3.37% at 0% RN down to 0.39% at 5% RN. This, however, is accompanied by a relatively higher percentage error in K_{12} estimates reaching 8.69% at 5% RN. Beyond 1% RN, estimates of K_{12} are almost independent of % RN up to 5% whereas those of K_{11} do improve at the expense of K_{12} as % RN increases.

This obviously indicates that SL_2-type phase diagrams precipitating SL_2-complexes produce better estimates of K_{12}, whereas those precipitating SL-complexes lead to better estimates of K_{11} at the expense of K_{12}, other factors being

Table II. The results of parameter estimates obtained from nonlinear least squares fitting of data for an SL_2-type phase solubility diagram (with an SL-complex precipitate) to which 0%, 1%, 2%, 3%, 4% and 5% random noise was superimposed. Those of S_o, S_M, T and K are the same as those in Table I

		Retrieved parameter estimates following nonlinear least squares fitting % Random noise (RN) superimposed					
Parameter	Input data	0%	1%	2%	3%	4%	5%
K_{11} (M^{-1})	100	103.3703	103.1582	102.3077	101.3703	100.5764	100.3928
(% error)		(3.37)	(3.16)	(2.31)	(1.37)	(0.58)	(0.39)
K_{12} (M^{-1})	70	68.76843	64.28281	64.02516	63.96883	63.9378	63.91777
(% error)		(1.76)	(8.17)	(8.54)	(8.62)	(8.67)	(8.69)

equal. Furthermore, it appears that good estimates of S_o do contribute largely to the precision of K_{11} and K_{12} obtained from the analysis of either regions I and III. In fact, those estimates deteriorate quite significantly as estimates of S_o vary slightly from linear fitting of region I, or from imprecise experimental measurements of S_o. Table III lists those estimates obtained from analysis of region I compared with those of region III for an SL_2-type system precipitating an SL_2-complex. It is seen that even for precise data (0% RN), a slight variation of S_o obtained from linear fitting of region I yields quite unreasonable estimates of K_{11} and K_{12} (69.22 instead of 100 for K_{11} and 16.81 instead of 70 for K_{12}). This occurs only for an estimate S_o = 0.00295 M compared with the true value of 0.00300. The corresponding estimates obtained from region III are much better (101.89 and 70.56 for 0% RN) approximating the true values quite well. However, as the % RN increases to 5%, values of K_{11} and K_{12} retrieved from region I become unreasonably wild leading to overestimates of K_{11} and negative values of K_{12} as % RN exceeds 3%. However, those obtained from region III stay within reasonable bounds of error even at 5% RN.

As for systems precipitating an SL-type complex, analysis of region I does provide better estimates of K_{11} than for an SL_2-complex precipitate as is shown in Table IV, but estimates of K_{12} are far off the true value becoming negative beyond 3% RN. Again, those obtained from analysis of region III remain within practically acceptable bounds of error.

Figure 4a shows the results of fitting region I according to Equation (8) for the same SL_2-type phase diagrams given in Figures 2b and 3b where 3% RN was superimposed. The solid line depicts precise data (0% RN) where S_o is also precisely defined. The line does appear quite linear as it should and leads to true estimates of K_{11} and K_{12}. The dashed line, however, represents a corresponding linear fitting of the scattered data points for the same region to which 3% RN was superimposed. Note the scatter of the data points around the dashed line yielding K_{11} = 1.70 instead of 100 and K_{12} = 28504 instead of 70. Therefore, it is safe

Table III. Comparison of partial formation constants estimated from region I with those obtained from nonlinear least squares fitting of region III for an SL_2-type phase solubility diagram (with an SL-complex precipitate) to which 0%, 1% , 2%, 3%, 4% and 5% random noise (RN) was superimposed.

Parameter	Parameter estimates from Region I		Parameter estimates from Region III	
	K_{11} (M^{-1}) (% error)	K_{12} (M^{-1}) (% error)	K_{11} (M^{-1}) (% error)	K_{12} (M^{-1}) (% error)
Input	100	70	100	70
0% RN	69.22	16.81	101.89	70.56
1% RN	68.50	263.75	101.75	66.90
2% RN	67.61	300.93	99.19	66.21
3% RN	1.70	285.04	97.69	65.82
4% RN	−33.00	−20.87	96.74	65.55
5% RN	−65.87	−13.42	95.50	65.21

Table IV. Comparison of partial formation constants estimated from region I with those obtained from nonlinear least squares fitting of region III for an SL_2-type phase solubility diagram (with an SL-complex precipitate) to which 0%, 1% , 2%, 3%, 4% and 5% random noise (RN) was superimposed

Parameter	Parameter estimates from Region I		Parameter estimates from Region III	
	K_{11} (M^{-1})	K_{12} (M^{-1})	K_{11} (M^{-1})	K_{12} (M^{-1})
Input	100	70	100	70
0% RN	116.52	32.78	103.77	68.77
1% RN	101.74	49.06	103.16	64.28
2% RN	112.90	7.31	102.31	64.03
3% RN	107.36	7.94	101.37	63.97
4% RN	110.45	−9.30	100.58	63.94
5% RN	113.70	−24.26	100.39	63.92

to conclude that analysis of region I according to Equation (8) becomes quite meaningless except for precisely measured data.

Figure 4b shows a plot of ($S_{eq}.L_{eq}$) against ($S_{eq}+L_{eq}$) according to Equation (26) for both systems shown in Figures 2a and 3a, respectively. The curve corresponding to region I is the same for both, but those of regions II and III are quite different. For systems precipitating an SL-complex, the curve of regions II and III appear almost linear with slight curvature extending along the same direction as that of region I. On the other hand, the corresponding curve for systems precipitating an SL_2-complex is quite nonlinear and appears inverted from that of region I. This is

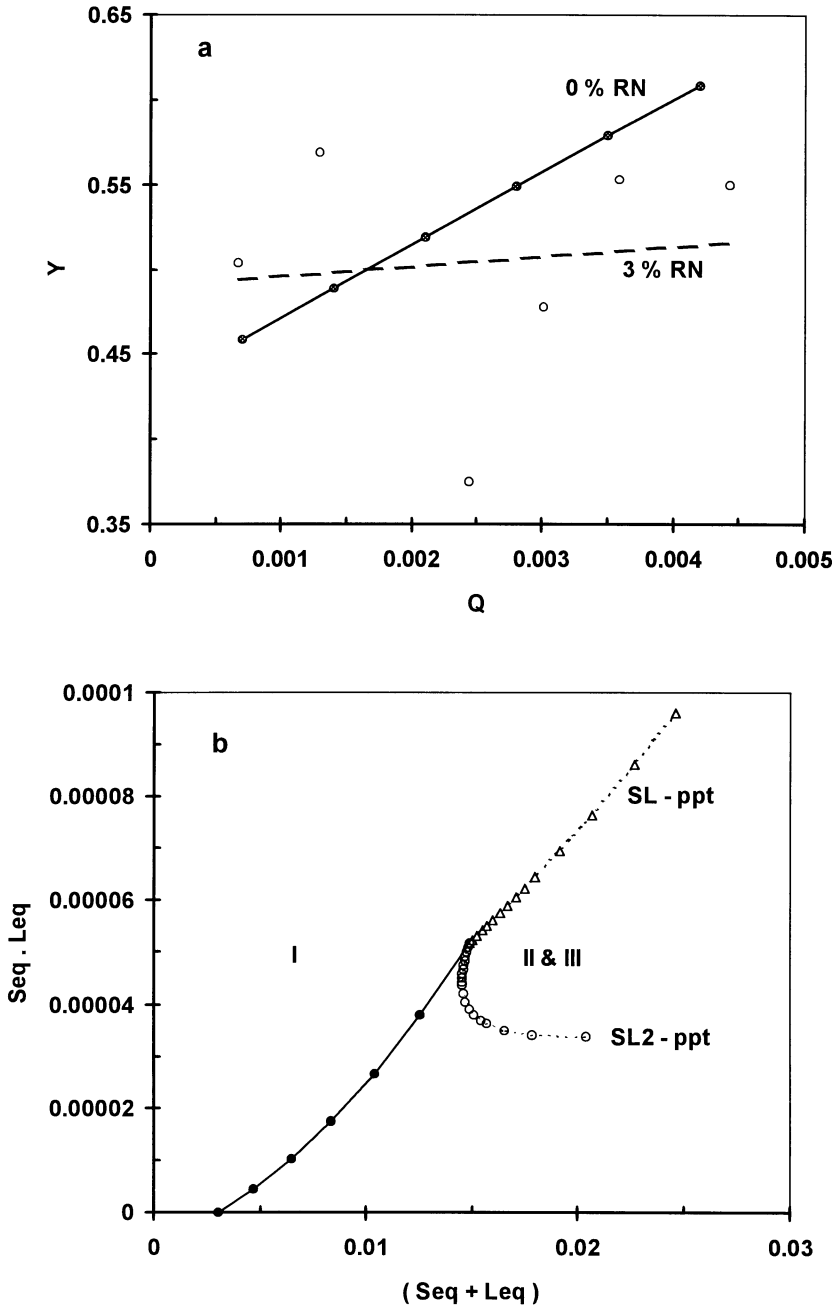

Figure 4. (a) A linear plot of Equation (8) for the rising portion (region I) of the phase diagram shown in Figure 2a. The solid line represents the best fit for precise data, whereas the dashed line with the scattered data points is what we obtain for the same region to which 3% random noise was superimposed. (b) A simple plot used to check which type of complex precipitates in regions II and III. The initial solid line represents data of region I. Each of the two dashed lines belong to regions II and III. The upper dashed line is almost linear for an SL-complex precipitate. The lower dashed line is always inverted from an extension of region I for an SL_2-complex precipitate.

a characteristic plot which can always be used to distinguish the type of complex reaching saturation first.

3.2. EXPERIMENTAL RESULTS

To illustrate the validity of this model used in the analysis of SL_2-type phase solubility diagrams, we have searched the literature for experimentally obtained diagrams that satisfy three criteria. First, diagrams should have enough data points in the rising and descending portions to make analysis meaningful. Second, the scatter in data of both regions should be as small as possible in order to ensure that true equilibria were clearly established between solute and solubilizer prior to solubility measurements. Third, the type of complex precipitate (SL or SL_2) should have been established by chemical or physical techniques. Among those found to satisfy the three criteria were the following solute/solubilizer systems:

1,3-Dimethylbenzoylurea (DMBU)/catechol in carbon tetrachloride [1], tolbutamide (Tolb)/β-cyclodextrin in water [5], spironolactone (SP)/γ-cyclodextrin in water [7], methylparaben (MP)/α-cyclodextrin in water, ethylparaben (EP)/α-cyclodextrin in water and propylparaben (PP)/α-cyclodextrin in water [2].

In each case, fitting of the experimental data was attempted first for an SL_2-type with an SL_2-complex precipitate (Equations (8) for region I, (13) for region II and (16)–(18) and (20) for region III), second for an SL_2-type with an SL-complex precipitate (Equations (8) for region I, (13) for region II and (23)–(25) and (18) for region III), and finally for an SL-type with an SL-complex precipitate (Equations (19) for region I, (29) for region II and (26)–(28) for region III). A unique convergence to one and only one of these three systems was arrived at in each case, within reasonable bounds of experimental error established using statistical significance tests for a 95% confidence level, and with confidence intervals on parameter estimates computed using the Student t-distribution.

The solubility of DMBU against catechol concentration in CCl_4 is reproduced from Higuchi and Connors [1] in Figure 5a. With S_o = (4.19 $\pm$ 0.6) $\times$ 10^{-3} M, analysis of region I yielded K = 21 $\pm$ 2 M^{-1}, while fitting data of region III only conformed to a system forming an SL-complex with no higher order complexes. The solid line in Figure 5a represents the best data fit obtained from linear regression of $(S_{eq}.L_{eq})$ against $(S_{eq} + L_{eq})$ according to Equation (26) yielding K_{11} = 24 $\pm$ 3 M^{-1} and K_{S11} = (6.9 $\pm$ 0.7) $\times$ 10^{-3} M^2. The corresponding plot is shown in Figure 5b; it is clearly linear with a K_{11} value agreeing well with that of K and thus excluding the possibility of formation of soluble higher order complexes. Attempted fitting of the data to an SL_2-type complex proved impossible for no convergence was attained. Parameter estimates thus obtained are listed in the second column of Table V.

Figure 6a shows the phase diagram reproduced for tolbutamide/β-cyclodextrin in water at 25 °C. The solid line represents the best possible fit which was only obtained for an SL_2-type complex with an SL_2-complex precipitate. The solubility

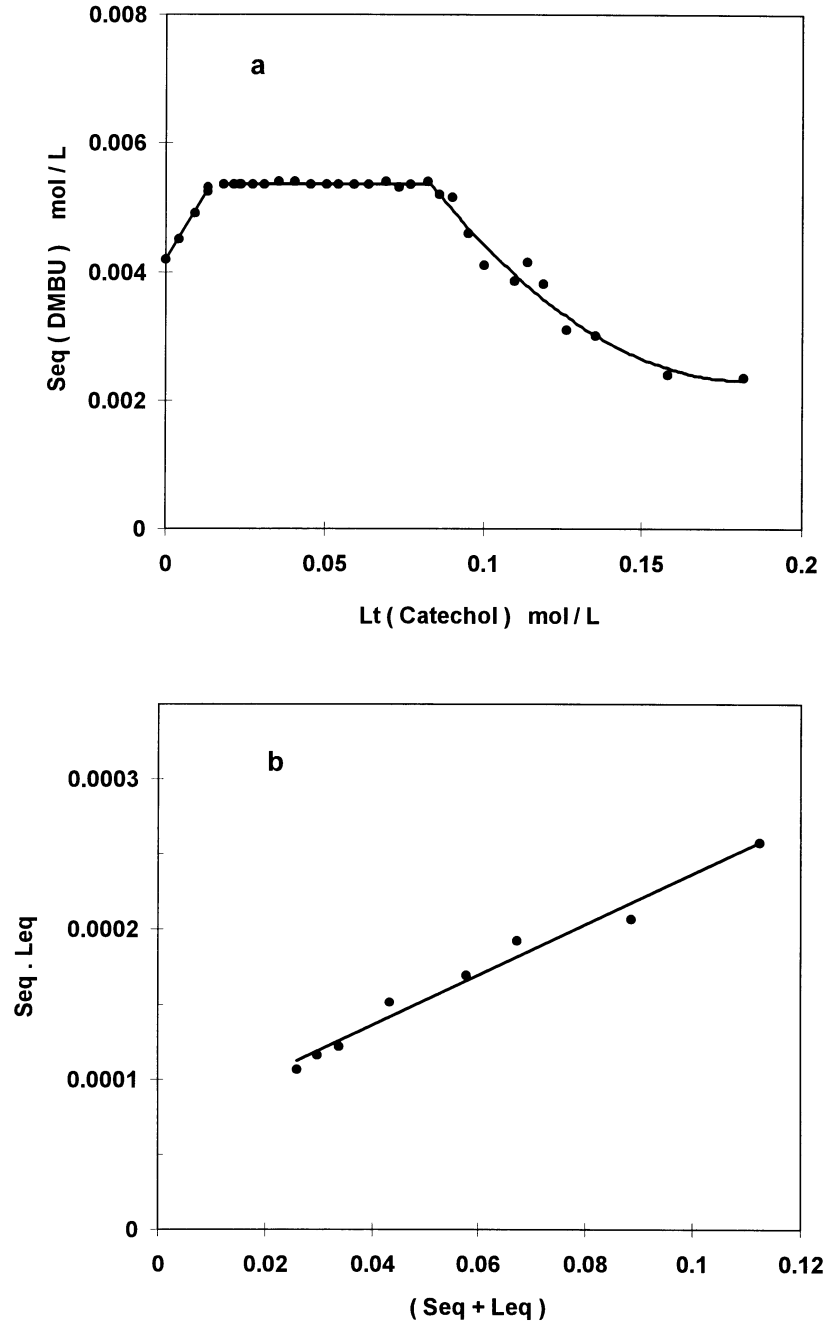

Figure 5. (a) Phase solubility diagram of 1,2-dimethylbenzoylurea against catechol concentration in carbon tetrachloride at 25 °C (Higuchi and Connors, 1965). (b) A linear plot of $S_{eq}L_{eq}$ against $(S_{eq} + L_{eq})$ for data of region III of the same phase diagram depicted in (a) showing that an SL-precipitate is formed.

Table V. Parameter estimates obtained from linear and nonlinear least squares fitting of experimental data reported in the literature on SL_2-type phase solubility diagrams with either SL- or SL_2-complex precipitates at 25 °C. [DMBU = 1,3-dimethylbenzoylurea, Tolb = Tolbutamide, MP = Methylparaben, EP = Ethylparaben, PP = Propylparaben, SP = Spironolactone, α-CD = α-Cyclodextrin, β-CD = β-Cyclodextrin, γ-CD = γ-Cyclodextrin]. Numbers in brackets next to each parameter denote confidence intervals estimated using the Student t-distribution for a 95% confidence level.

Solubility parameters	Solute/solubilizer system					
	DMBU/ catechol	Tolb/ β-CD	SP/ γ-CD	MP/ α-CD	EP/ α-CD	PP/ α-CD
Solvent	CCl_4	Water	Water	Water	Water	Water
Complex Precipitate	SL	SL_2	SL_2	SL	SL_2	SL_2
S_o	41.9	3.37	0.90	142	57.6	19.8
($\times 10^4$ M)	($\pm$0.6)	($\pm$0.23)	($\pm$0.03)	($\pm$3)	($\pm$3.2)	($\pm$2.4)
K	21	271	11140	221	174	214
(M^{-1})	($\pm$2)	($\pm$24)	($\pm$930)	$\pm$5)	($\pm$10)	($\pm$16)
K_{11}	24	221	8580	174	196	243
(M^{-1})	($\pm$3)	($\pm$18)	($\pm$320)	($\pm$8)	($\pm$7)	($\pm$13)
K_{12}		57	22	17	15	17
(M^{-1})		($\pm$6)	($\pm$2)	($\pm$4)	($\pm$2)	($\pm$5)
K_{S11}	6.9			2.5		
($\times 10^5$ M^2)	($\pm$0.7)			($\pm$0.2)		
K_{S12}		290	7.3		5700	2200
($\times 10^{10}$ M^3)		($\pm$17)	($\pm$0.2)		$\pm$200)	($\pm$300)
Data source	Higuchi & Connors (1965)	Kedzierewicz & *et al.* (1990)	Yusuff & *et al.*	Uekama York (1991)	Uekama *et al.* (1980)	Uekama *et al.* (1980)

parameters listed in the third column of Table V are: S_o = (3.37 $\pm$ 0.23) $\times$ 10^{-4} M, K = (271 $\pm$ 24) M^{-1}, K_{11} = (221 $\pm$ 18) M^{-1}, K_{12} = (57 $\pm$ 6) M^{-1} and K_{S12} = (2.90 $\pm$ 0.17) $\times$ 10^{-8} M^3. It is interesting to note that Kedzierewicz *et al.* [5] used a highly approximate relation suggested by Higuchi and Connors [1] for an estimation of $\beta_{12} = K_{11}K_{12}$ according to:

$$\beta_{mn} = S_B/\{(S_x - mS_B)(L_x - nS_B)\} \tag{31}$$

where S_B is the lowest solubility measured at the lower end of region III, S_x is the solubility at a given point along region III, L_x is the corresponding stoichiometric concentration of solubilizer at that point, while m and n denote the stoichiometric coefficients of the S_mL_n-complex precipitate. Using this relation the authors calculated a value for β_{12} = 2101 M^{-2}. This value is definitely not correct (our rigorous estimate is 12600 $\pm$ 2400 M^{-2}) since Equation (31) is highly approximate and always yields underestimates, and can only be used to obtain a rough estimate of β_{mn} when almost all free solute is practically removed from solution, and this is

obviously not the case demonstrated in Figure 6a. Earlier data reported by Uekama *et al.* [14] yielded only a value for K = 320 M^{-1} obtained from region I, which is not far off the 271 $\pm$ 24 M^{-1} obtained from those of Kedzierewicz *et al.* [5], but data of region II and III are different and could not be compared especially because the number of data points for region III was limited with much scatter in the earlier case to warrant meaningful analysis.

Figure 6b shows the phase diagram reported for spironolactone/γ-cyclodextrin in water at 25 °C. The solid line shows the only best possible fit obtained again for an SL_2-type complex with an SL_2-complex precipitate. The solubility parameters listed in the fourth column of Table V are: S_o = (9.0 $\pm$ 0.3) $\times$ 10^{-5} M, K = (11140 $\pm$ 930) M^{-1}, K_{11} = (8580 $\pm$ 320) M^{-1}, K_{12} = (22 $\pm$ 2) M^{-1} and K_{S12} = (7.3 $\pm$ 0.2) $\times$ 10^{-10} M^2: the estimate of K at 11140 M^{-1} was obtained assuming region I is linear, which clearly it is not, and is therefore meaningless. K_{12} may appear small in comparison with K_{11} but the contribution to SL_2-complex formation obtains from K_{11} through the overall formation constant $\beta_{12} = K_{11}K_{12}$ = (1.9 $\pm$ 0.2) $\times$ 10^5 M^{-2}.

Figure 7 depicts the phase diagrams reported by Uekama *et al.* [2] for methylparaben (MP), ethylparaben (EP) and propylparaben (PP) against α-cyclodextrin concentration in water at 25 °C. The solubility parameters obtained from the best possible fits of experimental data are listed in the last three columns of Table V. The strength of binding with α-cyclodextrin appears to increase steadily from MP to PP, indicating possible inclusion of the alkyl ester chain into cyclodextrin which might be more pronounced for PP (K_{11} =174, 196 and 243 M^{-1} for MP, EP and PP, respectively) than EP and MP. It must be noted however that among the three solutes which do form soluble SL_2-type complexes with α-cyclodextrin in solution, an SL-complex precipitates in the case of MP while an SL_2-complex precipitates in the other two (EP and PP). This corroborates the findings of Uekama *et al.* [2] concerning the type of complex precipitates obtained. However, their calculated values of K_{12} for EP and PP (using the approximate relation given by Equation (31)) are clearly overestimates. For example, they estimated K_{12} = 79 and 138 M^{-1} for EP and PP, respectively. The corresponding values obtained through our rigorous modeling were 15 $\pm$ 2 and 17 $\pm$ 5 M^{-1}, respectively. For the three closely related solutes, it is as yet unclear why an SL-complex precipitates in the case of MP while SL_2-complexes precipitate with EP and PP. This certainly merits some further studies, including molecular modeling to check whether inclusion of the benzene ring, through the hydroxyl group, is more energetically favorable for MP than either EP or PP, which may lead to the lower solubility of the SL-complex with MP. This must be contrasted, however, with the finding that K_{12}-values are almost equal for the three systems suggesting similar binding mechanisms between SL an L for the three solutes.

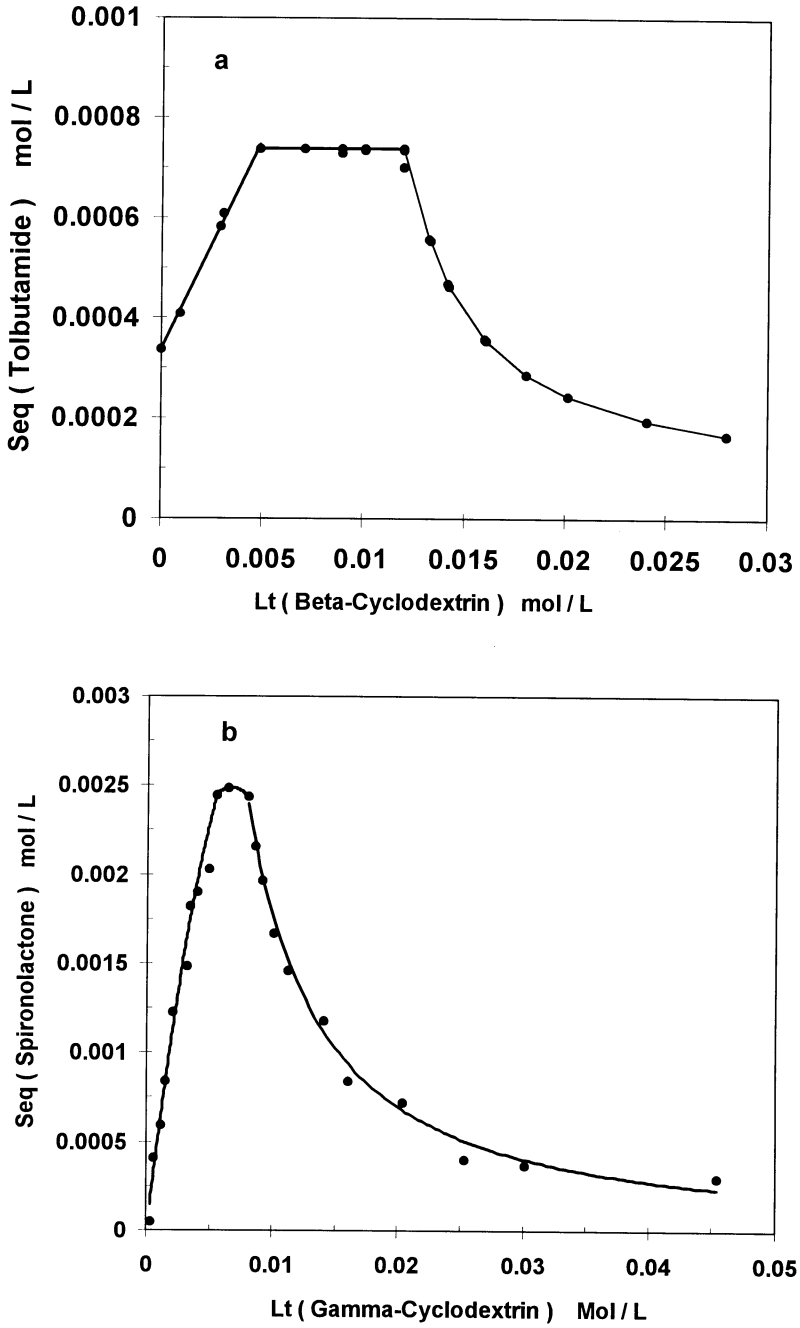

Figure 6. (a) Phase solubility diagram of tolbutamide against aqueous β-cyclodextrin concentration at room temperature (Kedzierewicz *et al.*, 1990). (b) Phase solubility diagram of spironolactone against aqueous γ-cyclodextrin concentration at 25 °C (Yusuff and York, 1991).

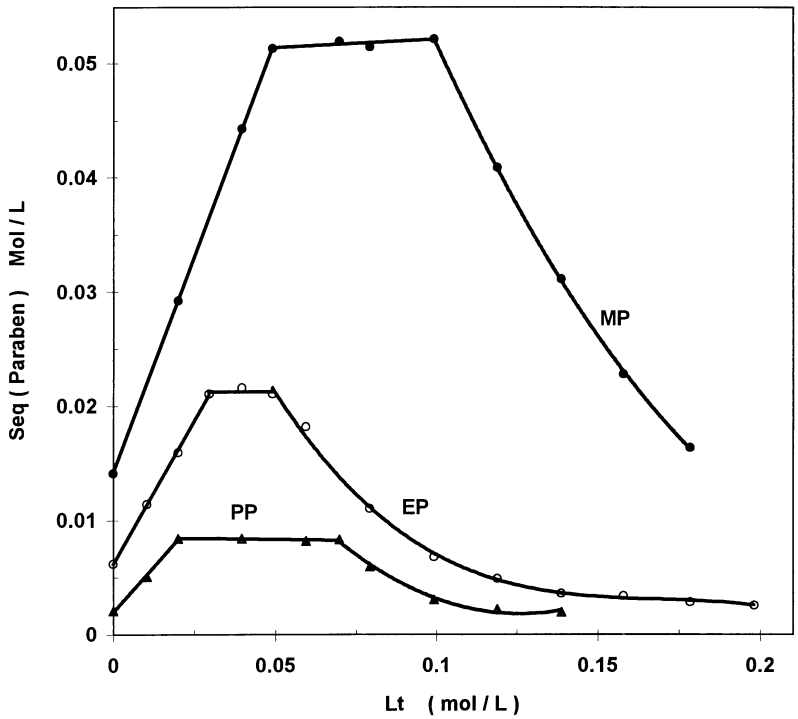

Figure 7. Phase solubility diagrams of methylparaben (MP), ethylparaben (EP) and propylparaben (PP) against aqueous β-cyclodextrin concentration at 25 °C (Uekama *et al.*, 1980).

4. Conclusions

In summary, the set of relations derived here allow rigorous fitting of experimental data to obtain meaningful estimates of individual complex formation and solubility product constants. Moreover, they offer the means to establish the type of complex precipitate from simple fitting of the descending portion of the phase diagram which has largely been ignored in the literature. The model has been thoroughly tested through computer simulation of experimental data, as well as on experimental data, and practical limits on the precision of experimental data required for reasonable estimates of solubility parameters were established.

Measurements of both S_{eq} and L_{eq} for each solution facilitate the analysis, but L_{eq} may be calculated from L_{t} through Equation (20) for an SL_2-type complex precipitate, or Equation (25) for an SL-type complex precipitate. The occurrence of regions I, II and III in the phase diagram results from the following experimental conditions:

Region I: The solid solute is present in excess at equilibrium with the solution where all complexes are soluble since none has reached saturation. Thus [S] = S_{o} and $S_{\text{t}} > S_{\text{eq}}$. Equation (8) may be used to obtain K_{11} and K_{12}, but this most often yields erroneous estimates unless highly precise data are obtained.

Region II: One of the two complexes reaches saturation and begins to precipitate. The solute is still present in excess and hence the free solute species remains fixed at [S] = S_o and so is the free solubilizer species [L] = [L_m]. The stoichiometric concentrations of all soluble species are all fixed and the system is invariant. This region (II) occurs when $S_t \geq S_m$ for $L_t > L_m$ and all data points along the plateau correspond essentially to a single point on an S_{eq} versus L_{eq} plot with the coordinate (S_m, L_m).

Region III: This must be an extension of the physical situation present in region II in so far as the type of complex precipitate is concerned. No new or higher order complexes precipitate or coprecipitate other than that of region II. Both free solute and free solubilizer species vary along region III which occurs subject to the condition $S_m < S_t < S_m + 0.5\,(L_t - L_m)$; $L_t > L_m$ for an SL_2-complex precipitate, and $S_m < S_t < S_m + (L_t - L_m)$ for an SL-complex precipitate.

The type of complex precipitate is ascertained through a plot of $(S_{eq}.L_{eq})$ against $(S_{eq} + L_{eq})$ according to Equation (26) for data of region III. If the complex precipitate is SL, the plot is almost linear extending from region I where L_{eq} is given by Equation (25). On the other hand, if the plot is inverted with respect to that of region I, the complex precipitate is SL_2 where L_{eq} is given by Equation (20). Finally, if the system forms only SL-type and no higher order complexes, then a plot of $(S_{eq}.L_{eq})$ against $(S_{eq} + L_{eq})$ according to Equation (26) will be exactly linear, with the values of K_{11} and K_{S11} obtained from Equations (28) and (27), respectively. K_{11} thus obtained will be equal to K that is obtained from Equation (19), while L_{eq} in this case will be given by Equation (30).

References

1. T. Higuchi and K. Connors: *Adv. Anal. Chem. Instr.* **4**, 117 (1965).
2. K. Uekama, Y. Ikeda, F. Hirayama, M. Otagin, and M. Shibata: *Yakugaku Zasshi* **100**, 994 (1980); *Chem. Abstr*. **94**, 398 (1981).
3. H. Seo, M. Tsuruoka, T. Hashimoto, T. Fujinaga, M. Otagiri, and K. Uekama: *Chem. Pharm. Bull.* **31**, 286 (1983).
4. Y. Takakura, K. Mon, M. Hashida, and H. Sezaki: *Chem. Pharm. Bull.* **34**, 1775 (1986).
5. F. Kedzierewicz, M. Hoffman, and P. Maincent: *Int. J. Pharm.* **58**, 221 (1990).
6. H.M.C. Marques, J. Hadgraft, and I.W. Kellaway *Int. J. Pharm.* **63**, 259 (1990).
7. N. Yusuff and P. York: *Int. J. Pharm.* **73**, 9 (1991).
8. S. Anguiano-Igea, F.J. Otero-Espinar, J.L.Vila-Jato, and J. Blanco-Mendez: *J. Pharm. Sci.* **2**, 325 (1992).
9. K. Iga, A. Hussain, and T. Kashihara: *J. Pharm. Sci*. **70**, 108 (1981).
10. K.A. Connors and D.D. Pendergast: *J. Am. Chem. Soc.* **106**, 7607 (1984).
11. K.A. Connors, A. Paulson, and D. Toledo-Velasque: *J. Org. Chem.* **53**, 2023 (1988).
12. F. Liu, D.O. Kildsig, and A.K. Mitra: *Pharm. Res.* **7**, 869 (1990).
13. M.B. Maurin, S.M. Rowe, C.A. Koval, and M.A. Hussain: *J. Pharm. Sci.* **83**, 1418 (1994).
14. K. Uekama, F. Hirayama, N. Matsu, and H. Koinuma: *Chem. Lett.* 703 (1978).
15. E.E. Sideris, G.N. Valsami, M.A. Koupparis, and P.E. Macheras: *Pharm. Res.* **9**, 1568 (1992).
16. M.B. Zughul and A.A. Badwan: *Int. J. Pharm.* **151**, 109 (1997).